Annals of Forest Science (2020) 77:99
https://doi.org/10.1007/s13595-020-01008-1

RESEARCH PAPER

Extended xylogenesis and stem biomass production in *Juniperus przewalskii* Kom. during extreme late-season climatic events

Junzhou Zhang[1,2,3] · M. Ross Alexander[2] · Xiaohua Gou[1,3] · Annie Deslauriers[4] · Patrick Fonti[5] · Fen Zhang[1,3] · Neil Pederson[2]

Received: 1 April 2020 / Accepted: 29 September 2020
© INRAE and Springer-Verlag France SAS, part of Springer Nature 2020

Abstract

• ***Key message*** **Late-season extreme climatic events induced variations in wood density and extended growth for more than a month in 2016 in *Juniperus przewalskii* Kom. growing on the Northeastern Tibetan Plateau, suggesting extraordinary growth resilience of the species in response to short extreme events over the cold and arid region.**

• ***Context*** Monitoring xylem formation (xylogenesis) during extreme meteorological events helps assessing climate change impacts on tree growth.

• ***Aims*** For better insight into tree-growth responses, here we compare the intra-annual formation of annual ring with and without intra-annual density fluctuation in *J. przewalskii* in a cold and arid environment on the Northeastern Tibetan Plateau.

• ***Methods*** Cambial phenology and xylogenesis observations of five mature trees during the 2016 intra-annual density fluctuation growth ring and the five-preceding year (2011–2015) were used for comparison. The frequency of population level occurrence of intra-annual density fluctuation in 2016 was examined on additional 50 randomly selected trees.

• ***Results*** The return of precipitation in conjunction with warm temperatures after summer drought promoted the growth resumption in 64% of our study trees, resulting in the observed intra-annual density fluctuation. These trees experienced a growing season 1 month longer than trees without intra-annual density fluctuation. The extended growth period resulted in a 17% increase in stem biomass in trees that experienced intra-annual density fluctuation.

• ***Conclusion*** Our results highlight the extraordinary resilience of *J. przewalskii* trees in response to extreme climatic events in the cold and dry conditions of the Tibetan Plateau.

Keywords Climate change · Drought · False rings · Resilience · Xylogenesis

Handling Editor: Cyrille B. K. Rathgeber

✉ Xiaohua Gou
xhgou@lzu.edu.cn

Junzhou Zhang
zhangjz@lzu.edu.cn

M. Ross Alexander
mrossalexander10@gmail.com

Annie Deslauriers
Annie_Deslauriers@uqac.ca

Patrick Fonti
patrick.fonti@wsl.ch

Fen Zhang
fzhang@lzu.edu.cn

Neil Pederson
neilpederson@fas.harvard.edu

[1] Key Laboratory of Western China's Environmental Systems (Ministry of Education), College of Earth and Environmental Sciences, Lanzhou University, Lanzhou 730000, China

[2] Harvard Forest, Harvard University, 324 North Main Street, Petersham, MA 01366, USA

[3] Gansu Liancheng Forest Ecosystem Field Observation and Research Station, Lanzhou 730333, China

[4] Département des Sciences Fondamentales, Université du Québec à Chicoutimi, 555 Boulevard de l'Université, Chicoutimi, QC G7H 2B1, Canada

[5] WSL Swiss Federal Research Institute, Landscape Dynamics, Birmensdorf, Switzerland

1 Introduction

Understanding how intra-annual tree growth responds to transient extreme meteorological events is important to better assess the impacts of future climate on tree growth (Fonti et al. 2010). The timing and duration of tree growth and the structure of the annual ring are environmental sensitive and thus respond to a large range of biotic and abiotic factors, including variations in temperature, precipitation, and extreme weather events (Deslauriers et al. 2017). Resolving the immediate tree response to weather conditions is timely also considering that climate projections suggesting important growing seasons shift and extensions due to climate warming (Rossi et al. 2016; Sanchez-Salguero et al. 2017). In addition, some regions could face alteration of the precipitation regimes with more frequent, intense, or longer droughts (Kumagai et al. 2004). Tree growth has been observed to be highly malleable in response to changing environmental conditions (Deslauriers et al. 2017), but it is not fully evident that trees in today's forests are resilient (adjust their growth to resume wood production) to the extreme weather conditions expected in the future. Studies that address these uncertainties via observations at the cellular level could have profound implications for a better mechanistic understanding of the growth processes. The consequences of such insight range from tree survival, species distributions, and the global carbon cycle (Fang et al. 2001; Pan et al. 2011).

Trees can respond to extreme climatic and weather events through a variety of structural adjustments or alterations of physiological processes. Some adaptations in the canopy include canopy dieback (McDowell and Allen 2015), changes in leaf function, or early leaf fall (Fernandez-de-Una et al. 2017). Some adaptations occur in the mechanisms that regulate stem growth (wood formation), including compensation for a shorter growing season with increased rates of cell production (Balducci et al. 2016; Cuny et al. 2019), decreasing the number of latewood cells (Wang et al. 2000), ceasing growth on one or more sides of the stem (Novak et al. 2016), or the cessation of cellular division under extreme water deficit (Deslauriers et al. 2016; Zhang et al. 2018). These kinds of plastic responses to extreme weather events in the cambium are reflected in the layering of xylem cells in radial growth rings through the number of cells produced or the anatomy of cells within a growth ring. When unfavorable climatic conditions occur, such as a severe summer drought, trees may initiate latewood cell formation (smaller lumen and thicker cell walls) well before the end of the growing season, reducing or even stopping cell division (Deslauriers et al. 2016). If there is a return of favorable conditions, trees can resume the production of earlywood-like tracheids with larger lumina and thinner walls (De Micco et al. 2016b). This intra-seasonal layering of earlywood-like tracheids after the creation of latewood tracheids, referred to as "false rings" (Schulman 1939) or intra-annual density fluctuations (IADFs), reflects important physiological processes and mechanical structures of tree responses to strong exogenous stimuli (De Micco et al. 2016b).

IADF formation has been frequently studied in the Mediterranean region where it is a common occurrence (De Micco et al. 2016b). Studies there have classified IADFs into two main types according to their relative position, within either the earlywood (E-type) or latewood (L-type) (Campelo et al. 2007; De Micco et al. 2016b). While E-type IADFs are related to conditions of extreme drought and high temperatures during the growing season, L-type IADFs are formed when the cambium reactivates under favorable late growing season conditions (Campelo et al. 2007; De Micco et al. 2016b). L-type IADF formation results in an extension of the wood formation period. Although IADFs have been observed in different environments around the world (Copenheaver et al. 2006; De Grandpré et al. 2011; Edmondson 2010; Marchand and Filion 2012; Masiokas and Villalba 2004), reports of IADF formation and potential formation mechanisms are much less frequent outside of the Mediterranean region. Therefore, further studies are needed to increase our understanding of IADF formation in other environments.

Most studies of IADFs have been conducted indirectly through the extraction of growth rings by increment coring, where correlations are made between years with the presence of IADFs and a range of climate variables (Battipaglia et al. 2016; Campelo et al. 2007). While these studies can identify the potential conditions or extreme climatic events leading to IADF formation, interpretations of what drives IADF formation can be uncertain. By sampling tree stems every 1–2 weeks, so-called microcoring, researchers can more precisely identify periods of cell production throughout the growing season (Fonti et al. 2010). Microcoring, therefore, provides better insight into the precise timing of xylogenesis and a more direct and precise temporal investigation of what drives IADF formation (De Micco et al. 2016a). A few studies have applied these direct and frequent observations of xylogenesis to investigate IADF formation (Balzano et al. 2018; De Micco et al. 2016a). However, there is still much to learn about how other tree species and other environments respond to changes in the timing and structure of the growing season and extreme weather events in many different tree species and in many of the world's forests.

In this study, we monitored the formation of the annual rings of *Juniperus przewalskii* Kom. trees during 2011–2016 with and without IADF formation in a cold and arid environment on the northeastern Tibetan Plateau. Specifically, we intend to (1) characterize the process of IADF formation, (2) identify its main drivers, and (3) assess its frequency of occurrence and (4) potential impacts on biomass productivity. We tested the hypothesis that the IADF formation in

J. przewalskii, like observed in some Mediterranean species, is a plastic response mechanism to favorable growth conditions that follow an unfavorable period.

2 Materials and methods

2.1 Study site

Our study site is located at 3100 m above sea level (asl) in the Tulugou National Forest Park (36° 43′ 21″ N, 103° 37′ 59″ E) of the northeastern Tibetan Plateau (Fig. 1a). As recorded by an on-site meteorological station (HOBO U30, Onset, USA) from 2011 to 2016, local climate is characterized by a mean annual temperature of 1.7 °C and an annual precipitation sum of 699 mm, indicating an arid and cold climate (Fig. 1b). Our study forest is composed of *J. przewalskii* trees growing at the upper forest limit on a dry, infertile, and south-facing slope. Our study trees are mature, 6 to 9 m tall, and have a stem diameter at breast height (DBH) between 15 and 30 cm. As typical for steppe forests, canopy cover is less than 20%.

2.2 Microcore collection, preparation, and observation

Observations of xylem development were performed of five dominant mature trees without substantial damages or anomalies. Selected trees were upright, 64 ± 7 years old, 6.3 ± 0.5 m tall, and displayed an average DBH of 24.2 ± 3.0 cm. Observations were based on repeated microcoring using a Trephor (Rossi et al. 2006). Microcores were taken at stem breast height (1.3 m) weekly (2011–2014) or biweekly (2015–2016) from mid-April until the end of September. Three microcores were taken from each tree in each sampling date (see Zhang et al. 2018 for details). Immediately after collection, microcores were stored in a solution of formalin, alcohol, and acetic acid on a 5:90:5 ratio. In the laboratory, microcores were softened in 70% alcohol and glycerin solution (1:1), dehydrated in ethanol, cleaned in dimethylbenzene, and embedded in paraffin. Transverse sections of 12-μm thickness were cut with a rotary microtome (RM 2245, Leica, Germany), stained with safranin (1% in water) and fast green (0.5% in 95% ethanol), and photographed under an optical microscope at 100–400 of magnification (bright field and polarized light).

We counted the number of cambial, enlargement, wall thickening, and mature cells on each micro-section along three radial rows. Cambial cells had rectangular shape, small radial diameters, and thin primary walls. During the enlargement phase, cells were at least two times larger than cambial cells and had thin walls that were not birefringent under polarized light. Wall thickening cells were distinguished by the birefringence of the oriented microfibrils within the secondary walls under polarized light (Abe et al. 1997). Mature cells had lignified walls without protoplasts, and the walls were completely stained red by saffron and fast green counterstaining (Zhang et al. 2013).

Xylem development was characterized via timing of relevant phenological phases. Specifically, we annotated the day of the year (DOY) corresponding to the onset and cessation of cell enlargement (here defined as duration of cell production) and the end of cell maturation (corresponding to the end of xylogenesis). However, since we observed a bimodal growth with formation of IADF in 2016, we also annotated the second onset and ending of cell enlargement in IADF trees (i.e., corresponding to the second growing mode). The daily mean growth rate was simply calculated as the ratio of the total number of xylem cells produced during the growing season and the duration of cell production.

2.3 IADF occurrence

To assess the occurrence of IADF at the population level, we made a collection of tree-core samples from 50 randomly selected trees around our microcored trees using an increment borer in 2018. Core samples were extracted at breast height

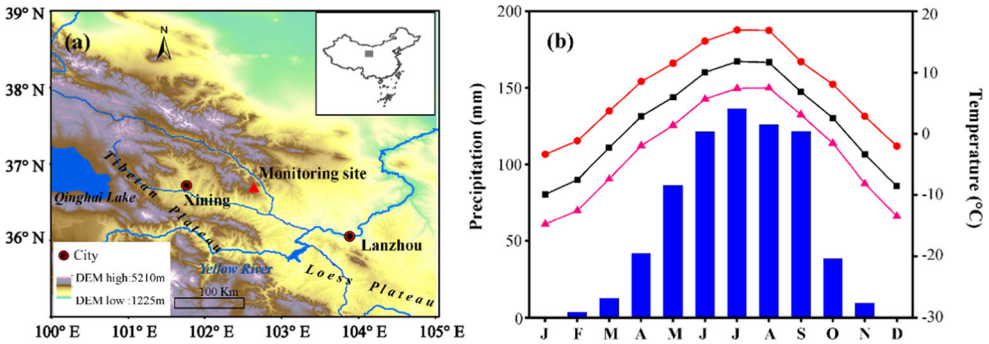

Fig. 1 **a** Location of monitoring site (red triangle). The study region is the intersection region between the Loess Plateau (southeastern) and the Tibetan Plateau (southwestern). **b** Distribution of the monthly mean (black square), maximum (red circle), and minimum (pink triangle) temperature and precipitation (blue bar) during the period of 2011–2016 from the on-site meteorological station

(1.3 m) from each tree in four different directions. All the samples were mounted, air-dried, and sanded to facilitate annual ring identification (Stokes and Smiley 1968). Rings were crossdated and IADFs were identified under a microscope. Total ring width and the ring width before IADF formation in 2016 were measured to the nearest 0.001 mm using a Velmex measuring system. The ring width after IADF formation was calculated as the difference between the total ring width and the width before IADF formation. The boundary between the IADF was defined as the location with a sudden change in cell size, lumen size, and color. DBHs were also collected from all cored trees.

2.4 Meteorological data

To identify the driving climatic factors inducing IADF, we used daily data from the on-site meteorological station recording air temperature, precipitation, relative humidity, soil temperature, and soil water content at 10-cm depth at 10-min resolution from 2011 to 2016.

2.5 Stem biomass estimation

To estimate the additional stem biomass associated with the IADF formation, we used allometric equations to assess the amount of wood produced in the year 2016. Because there were no reported allometric equations for *J. przewalskii*, we estimated the stem biomass (*Bst*) using the allometric equation for a species with similar architecture, *Juniperus thurifera* (García Morote et al. 2012):

$$ln\,(Bst) = -1.53 + 1.80\,ln\,(DBH)$$

The stem biomass associated with IADF formation was estimated as the difference between total of biomass with the growth and before IADF formation:

$$Bst_{\mathrm{IADF}} = e^{[-1.53+1.80\ ln\ (DBH+2\mathrm{rwt})]} - e^{[-1.53+1.80\ ln\ (DBH+2\mathrm{rwb})]}$$

where Bst_{IADF} is the stem biomass associated with IADF formation, rw_b indicates the ring width before IADF formation, and rw_t means the total ring width of 2016.

3 Results

3.1 The climatic peculiarity of the 2016 growing season

In 2016, both mean annual temperature and total precipitation were slightly higher than those in the previous 5 years (2.2 °C in 2016 versus an average of 1.6 °C from 2011 to 2015 and 732.2 mm in 2016 versus an average of 692 mm from 2011 to 2015, respectively). However, the distribution of precipitation during the 2016 growing season was substantially different. In 2016, there was no precipitation for the 16 days between July 29 and August 13 (DOY 211-226), resulting in the lowest soil water content of the growing season (Fig. 2a). At the same time, average mean temperature during the 16-day drought was higher than any measured mean from 2011 to 2015 (15.5 °C in 2016 versus a mean of 12.3 °C from 2011 to 2015). The warm and dry period of 2016 ended on August 14 (DOY 227) with the largest amount of daily precipitation (30.8 mm) of the year. After the downpour of August 14, the following 38 days saw relatively large and rather frequent rainfall events, which made September 2016 the wettest month of the year. At the same time, daily mean temperatures did not drop below 6.1 °C until September 19 (DOY 262). Previously, the date when daily mean temperature first dropped below 6.1 °C from 2011 to 2015 ranged from Sept. 1 in 2012 to Sept. 14 in 2014. The meteorological we collected underscore that 2016 was an unusually dynamic late season compared to the previous 5 years at our study site.

3.2 Xylogenesis

Although the timing and duration of xylogenesis varied significantly among the first 5 years (2011–2015) (Fig. 2b), the period of cell production typically occurred between May 2 (DOY 122, in 2013) and August 4 (DOY 216, in 2011), and tracheid maturation maximally extended to September 7 (DOY 250, in 2011). The longest duration of cell production was in 2011 and covered 79 days (from May 18 to August 4 (DOY 138-216)) while 2012 showed the shortest duration of cell production (55 days from May 28 to July 21 (DOY 149-203)). When including the period of maturation, the longest observed growing season was also in 2011 (113 days, from May 18 to September 7 (DOY 138-250)). The shortest observed growing season (87 days) occurred in 2014 and lasted from May 22 to August 16 (DOY 142-228).

Xylogenesis in 2016 showed a different pattern than compared to the previous 5 years. Two trees followed the patterns and timing of xylogenesis observed during the previous 5 years. However, three trees showed a bimodal growth pattern that included the formation of IADF and an extended growing season (Fig. 3). The onset of cell production in 2016 for all five trees was rather synchronous and started around May 18 (DOY 139) (Figs. 2b and 4). And, like the two trees without IADF, cell production of the three IADF trees was complete by August 3 (DOY 216). From there, the xylogenesis of these two populations diverged. While all xylem cells in the two non-IADF trees matured by September 2 (DOY 246, Fig. 4(b)), the three IADF trees showed new growth, the production of earlywood-like enlarging, and wall thickening cells on August 16 (DOY 229, Fig. 4(b, c)). Based on our samples and analyses, one can logically conclude that IADFs developed in these trees sometime between August 3

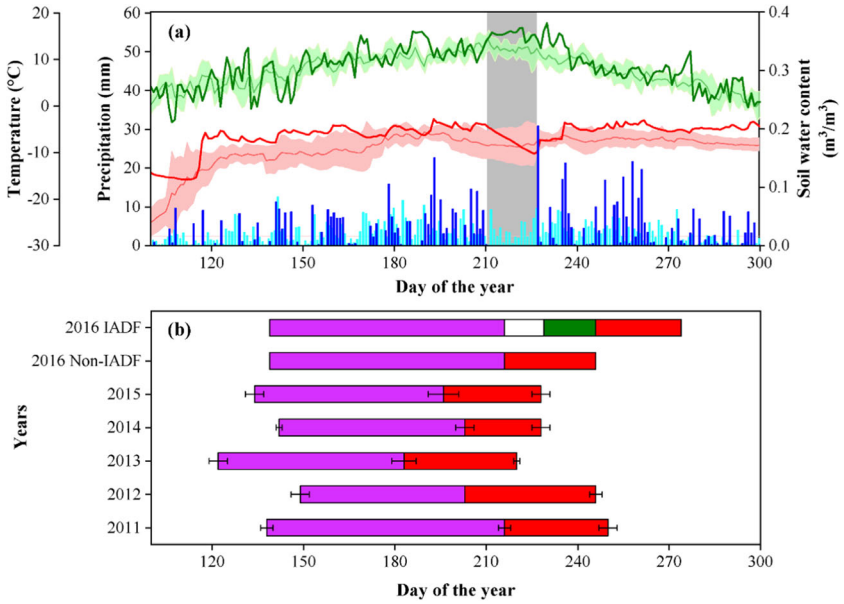

Fig. 2 **a** Comparisons of daily temperature in 2016 (wide green line) and 2011–2015 mean ± SD (thin green line with green shaded area), soil water content in 2016 (wide red line) and 2011–2015 mean ± SD (thin red line with red shaded area), and precipitation in 2016 (blue vertical bars) and 2011–2015 mean (light blue vertical bars). The gray-shaded area illustrates the 16-day period, from July 29 through August 13, without any measurable precipitation. **b** Cambial phenology during the 2011–2016 growing season. The beginning and end of pink horizontal bars indicate the timing of onset and end of cell enlargement, respectively (i.e., the first cell production phase); the end of red horizontal bars indicate the end of cell maturation (i.e., the end of growing season); and the beginning and end of green horizontal bar indicates the second onset and end of cell enlargement (the second cell production phase) of the intra-annual density fluctuation (IADF) trees in 2016 growing season. Error bars indicate the mean ± SD

and August 16 (Figs. 2–4). The season of cell production in the trees with IADF formation was completed between September 2 (DOY 246) and September 13 (DOY 257), which is more than a month later than the two non-IADF trees. Termination of cell wall lignification in the three trees with IADF formation occurred around our last sampling date, September 30.

Even though peak cell production in both trees with and without IADFs occurred in early June (DOY 167), a comparison of phases in cell developmental between these groups indicated a higher number of cambial cells (Fig. 4) and a significantly higher mean rate of cell production in IADF trees than in non-IADF trees (Fig. 5b). Both groups also stopped cell division (i.e., the number of enlargement cells dropped to zero) by August 3 (Figs. 3 and 4). Cell division resumed in the IADF trees where an average of 2.4 ± 0.8 enlarging earlywood-like cells and 1.7 ± 0.1 latewood-like cells was observed among the three trees on August 16 and September 2, respectively. The number of wall-thickening cells was higher in IADF trees than in non-IADF trees before August 3, when all the trees first stopped cell production.

The total number of xylem cells produced each year was variable over the course of our 6 years of observation. The highest level of cell production occurred in 2012 and reached a mean of 42 cells, which is twice the value for 2015, which registered only a mean of 21 cells (Zhang 2018). Notably for 2016 and much like the minimum and maximum values of xylem cell production over our 6 years of observations, trees with IADFs showed a high total number of produced xylem cells that was approximately twice that of non-IADF trees (39 ± 6 cells vs. 21 ± 5 cells).

3.3 IADF occurrence and extra biomass production

Our tree-coring campaign in the forest surrounding our five micro-cored trees showed that 32 out of 50 trees formed IADFs within the 2016 annual growth ring (Table 2). This proportion (64%) confirms the rate of IADF formation observed on the xylogenesis trees (60%). Similar to findings in the micro-cored trees, increment-cored trees with IADFs had a higher mean growth rate, and produced more cells (Fig. 5a–c) and a wider 2016 ring (Fig. 5d) than non-IADF trees. Interestingly, the average DBH of trees with IADFs was slightly smaller than that of non-IADF trees, both in micro-cored trees and in increment-cored trees (Fig. 5a).

The extra growth observed in trees with IADFs resulted in extra biomass production. Micro-cored IADF trees, with a mean of 5.3 ± 0.5 additional xylem cells, yielded a mean radial increase of 169 ± 17 μm and a mean increase of 17.2 ± 4.3% of xylem cells (Table 1). Similarly, a mean of 161 ± 58 μm of additional ring width was measured in the 32 increment-cored trees with IADFs in 2016. This additional IADF-related growth resulted in a mean increase of 17.4 ± 9.5% of radial increment (Table 2). Translating IADF-related growth into

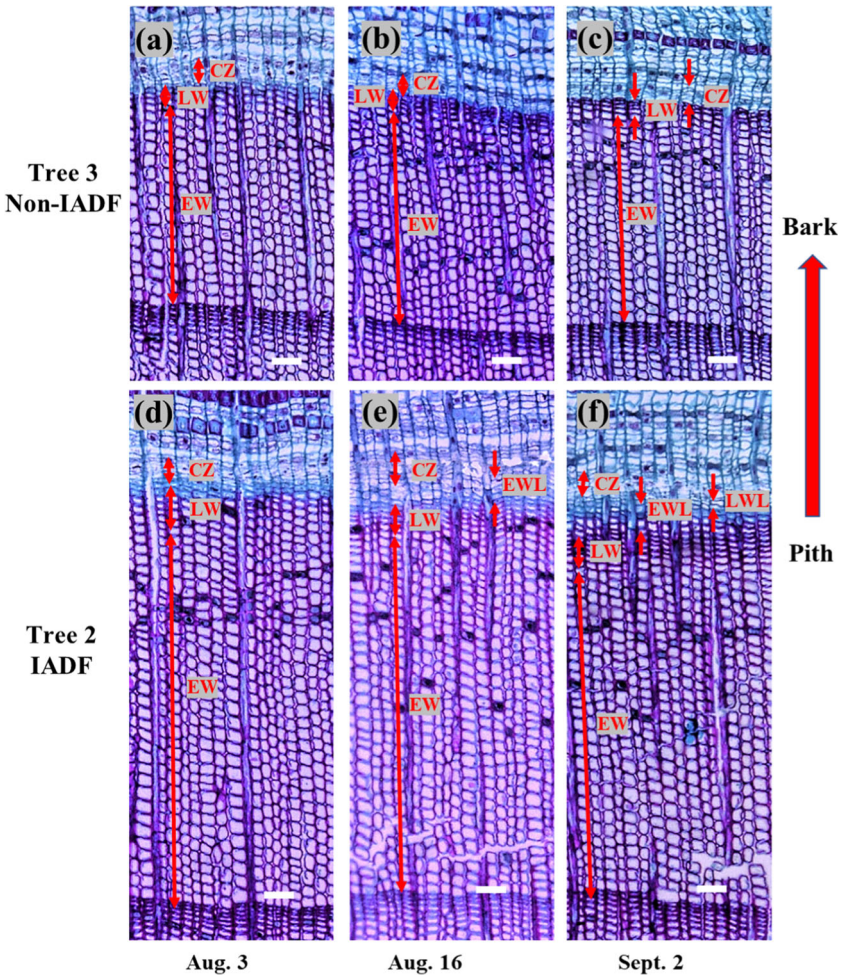

Fig. 3 Wood formation of trees without (tree 3) and with (tree 2) intra-annual density fluctuation (IADF) formation. Cells have been double stained with red tones indicating mature xylem cells and blue tones indicating developing xylem cells and phloem cells. For the trees without IADF formation, the end of cell production (associated the end of cell enlargement phase) was observed on August 3 (DOY 216) (**a**), the lignification of xylem cells continues on August 16 (DOY 229) (**b**), and all the cells matured on September 2 (DOY 246) (**c**). For the trees with IADF formation, the first ending of cell production (associated the end of cell enlargement phase) was observed on August 3 (DOY 216) (**d**); however, wood production was followed again by earlywood-like cells and first observed on August 16 (DOY 229) (**e**), and the second end of cell production observed on September 2, DOY 246 (**f**). The white bar in each image represents 50 μm. CZ, cambial zone; EW, earlywood; LW, latewood; EWL, earlywood-like cells; LWL, latewood-like cells

biomass showed a net increase of 0.14 ± 0.02 kg, which corresponds to a + 18.1 ± 4.7% of wood production in micro-cored trees (Table 1, Fig. 6). Similar values were calculated for the 32 increment-cored IADF trees (0.12 ± 0.06 kg, i.e., +16.9 ± 8.7%; Table 2, Fig. 6).

4 Discussion

Our observations indicated that 60–64% of *J. przewalskii* trees in our study forest showed a resumption of cambial growth after a growth cessation in August 2016. The bimodal growth pattern resulted in annual rings that contained variations in cell structure and wood density within the latewood of the growth ring, aka, L-type IADFs (Campelo et al. 2007). To the best of our knowledge, this is the first time that this kind of post-growing season L-type IADF formation has been observed in continental environment as cool and dry as the Tibetan Plateau. Remarkably, we observed that a majority of the study population trees were able to extend cambial growth for more than a month longer than previously observed.

4.1 Potential cause of IADF formation

Two processes are required to generate an IADF. The first is a slow-down or cessation in the processes driving cambial growth. The second is a resumption of growth after the initial cessation (Popkova et al. 2018; Vieira et al. 2014). In this study, we observed a reduction of cell production concurrent with the warm dry spell in early August, confirming our prior work that a reduction in water availability during summer can induce the end of cell production (Zhang et al. 2018). Given the evidence presented above and our prior experience with this system, the combination of a warm and dry early August likely anticipated growth termination of cell production in 2016. However, the growth resumption with a production of new earlywood-like cells occurred concurrently with the resumption occurrence of rather frequent and relatively large rainfall events. Therefore, the intense precipitation dynamics of mid-August under favorable warm temperatures very likely contributed to the IADF formation, at least for the trees that were vital enough to resume growth (Popkova et al. 2018).

Our findings indicate that the growth of our *J. przewalskii* was limited by a lack of cell turgor, even though cambial cell

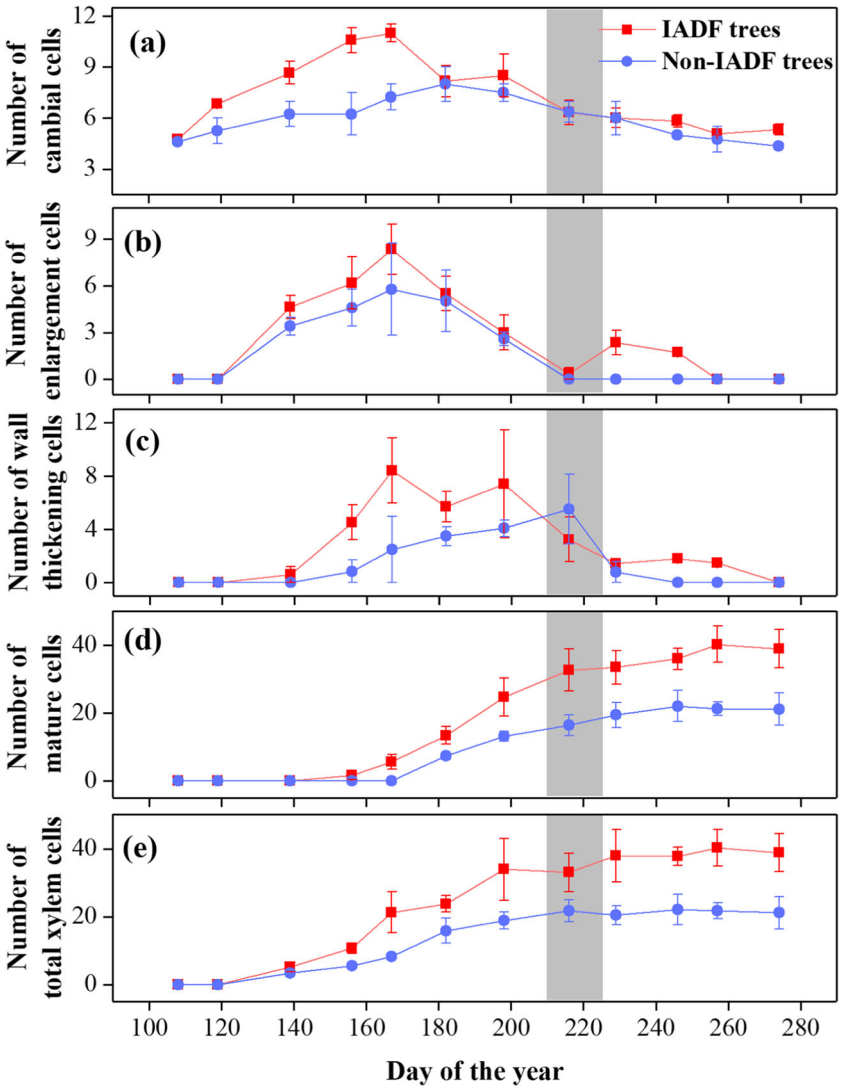

Fig. 4 Number of cells in different development stages of xylogenesis in the trees with intra-annual density fluctuation (IADF) (squares) and without IADF (circles) formation throughout the 2016 growing season. Error bars indicate the mean ± SE; the gray-shaded area in each panel illustrates the 16-day period, from July 29 through August 13, without any measurable precipitation

division and differentiation can require high levels of sucrose from photosynthesis (Deslauriers et al. 2016; Oribe et al. 2003). Drought can directly impact cambial activity earlier than indirectly via the reduction of photosynthesis under drought stress (Muller et al. 2011). This relationship mirrors Deslauriers et al. (2016), who found that cell division ceases when irrigation ceases. In fact, we found that the photosynthetic rate of *J. przewalskii* from 2011 to 2016 at our study site was higher during the end of cell production (Zhang 2018), supporting that newly assimilated carbon is not the main factor determining the cessation and resumption of wood production.

Our results support the hypothesis that the L-type IADFs observed in this study follow the similar mechanism described in trees living in the Mediterranean climate, i.e., that late growing season precipitation plays a crucial role for IADF formation (De Micco et al. 2016b). However, we cannot ignore the role of mild temperatures in the formation of IADFs in the cold Tibetan Plateau. Our investigations on these same trees show that radial growth can continue as long as the daily mean temperature remains above 6.1 °C and if there is sufficient precipitation (Zhang 2018). The warm conditions under which the resumption of rainfall occurred from mid-August through late September 2016, it is likely that tree water status was restored enough to resume cambial cell division and enlargement, as it can happen for the onset of xylogenesis in *J. przewalskii* has been described to be driven by an interaction of temperature and precipitation (Ren et al. 2018). Therefore, both the return of precipitation and the occurrence of warm conditions were vital for the resumption of new earlywood-like cells after the cessation in summer. In this case, the role of warm temperature on the L-type IADF formation in the annual ring is slightly different from the IADF formation in the Mediterranean region (Battipaglia et al. 2010b; Novak et al. 2013). These results highlight the great plasticity in growth response to extreme, transient meteorological events of this species.

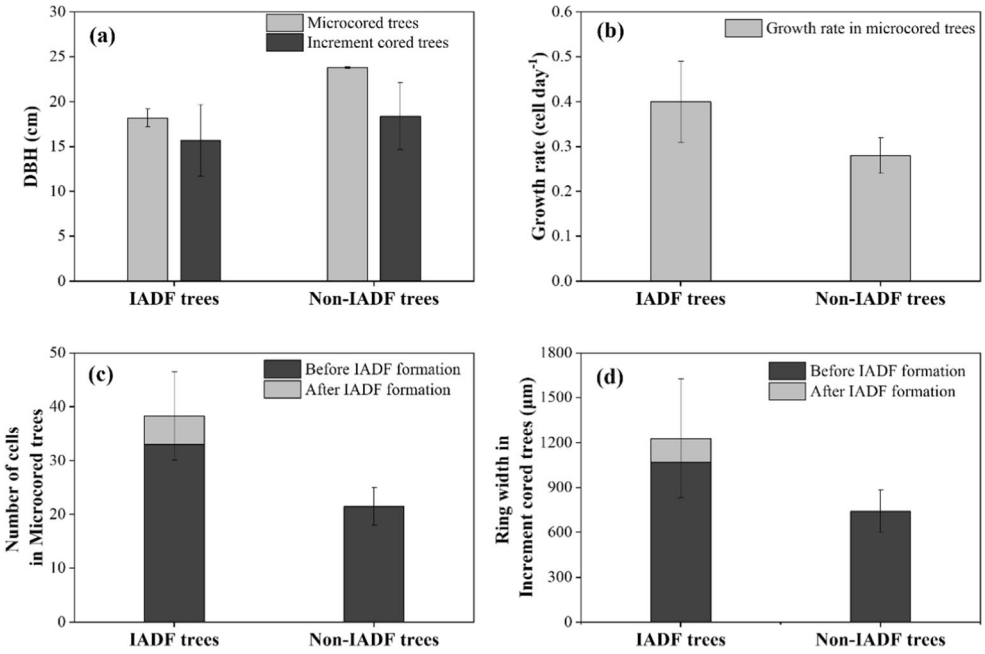

Fig. 5 Comparisons of diameter at breast height (DBH; **a**), mean growth rate (**b**), the number of cells in micro-cored trees (**c**), and ring width in increment-cored trees (**d**) between IADF trees and non-IADF trees

4.2 Ecological implications of the IADF-related extended growing season

Our results showed that the majority of IADFs were formed in wider rings or observed in smaller trees, indicating that smaller trees or trees with wider rings were more sensitive to extreme meteorological events and thus more vigorous. These results also confirm previous observations of higher frequency of IADF in wider rings (Battipaglia et al. 2010a; Campelo et al. 2013) and, often, younger or smaller trees (Popkova et al. 2018; Rigling et al. 2001). Considering xylem cell production as an indicator of tree vigor, a higher xylem cell production could thus indicate higher growth resilience to unfavorable conditions and stronger capacity to resuming growth when the conditions return favorable. However, it is also possible that microsite conditions could also play an important role in regulating the resilience capacity. Microsite conditions at the dry, cool margin of growth have been shown to greatly affect the climatic response of trees (Bunn et al. 2005). Our observations support the call for continued integration of disciplines to understand the biotic and abiotic factors behind tree growth in extreme sites (Lloyd et al. 2017).

The occurrence of IADF in the dry and cold environment highlights the great phenological and growth plasticity of *J. przewalskii* to resiliently respond to short extreme events. Although future projections for the northeastern Tibetan Plateau indicate a trend towards a warmer, wetter climate, the seasonality of precipitation is uncertain (Gou et al. 2015) and events like the 2016 extreme drought could become more frequent. Based on our xylogenesis and additional documentation of frequent IADF formation across the larger tree population, we suspect that a substantial portion of the *J. przewalskii* on the northeast Tibetan Plateau might not simply stop cambial growth during a drought like that in 2016, but

Table 1 Information of intra-annual density fluctuation (IADF) formation in micro-cored trees. The number of xylem cells before (cn_b) and after (cn_a) IADF formation, corresponding ring width before (rw_b) and after (rw_a) IADF formation and their total (rw_t) were presented; Bst_{IADF} indicates the extra stem biomass when IADF formation; *% increase* means percent increase in stem biomass when IADF formation (%)

Tree identifier	DBH (cm)	cn_b	cn_a	rw_b (μm)	rw_a (μm)	rw_t (μm)	Bst_{IADF} (kg)	% increase
M1	23.7	18.0	–	548	–	548	–	–
M2	16.9	41.0	5.0	1235	153	1388	0.116	12.5
M3	23.9	25.0	–	762	–	762	–	–
M4	18.4	36.0	6.0	1084	192	1276	0.156	17.8
M5	19.4	22.0	5.0	679	162	841	0.136	23.9
Mean	20.5	28.4	5.3	862	169	963	0.136	18.1
SD	2.8	8.7	0.5	257	17	318	0.016	4.7

Table 2 Information of intra-annual density fluctuation (IADF) formation in increment coring trees. The ring width before (rw_b) and after (rw_a) IADF formation and their total (rw_t) were presented; Bst_{IADF} indicates the extra stem biomass when IADF formation; *% increase* means percent increase in stem biomass when IADF formation (%)

Tree identifier	DBH (cm)	rw_b (μm)	rw_a (μm)	rw_t (μm)	Bst_{IADF} (kg)	% increase
I02	24.7	1620	219	1839	0.225	13.6
I04	15.3	504	153	657	0.106	30.5
I05	15.6	532	242	773	0.276	33.1
I06	13.4	842	138	980	0.091	15.7
I07	10.8	1039	192	1231	0.102	18.6
I08	16.7	807	199	1006	0.248	14.9
I09	17.0	1094	219	1313	0.166	20.1
I10	15.5	837	177	1015	0.125	25.1
I11	14.1	1774	171	1945	0.097	11.3
I14	20.0	1135	154	1289	0.133	13.7
I15	16.5	785	114	899	0.084	14.6
I16	13.8	693	89	782	0.057	12.9
I18	16.9	2076	147	2222	0.112	7.2
I20	9.8	851	66	917	0.032	8.2
I21	14.2	1353	177	1530	0.117	13.2
I22	17.8	790	180	970	0.141	22.9
I23	16.0	1616	122	1738	0.088	7.6
I24	17.4	1088	237	1325	0.184	21.9
I25	5.3	557	72	629	0.022	13.0
I27	14.1	721	315	1036	0.205	43.9
I28	13.8	1239	119	1358	0.097	8.3
I30	17.2	1325	98	1423	0.075	7.4
I32	11.7	955	81	1036	0.046	8.5
I35	15.5	1296	138	1434	0.093	12.8
I36	7.5	783	127	910	0.050	16.4
I38	20.2	1518	84	1602	0.073	5.6
I39	22.9	1092	113	1205	0.104	10.9
I40	21.0	614	164	778	0.147	26.8
I44	16.2	785	180	965	0.131	23.0
I46	15.2	1417	233	1650	0.163	17.1
I48	15.7	808	234	1042	0.167	30.0
I49	20.6	1625	195	1820	0.173	12.1
Mean	15.7	1068	161	1229	0.123	16.9
SD	4.0	393	58	396	0.060	8.7

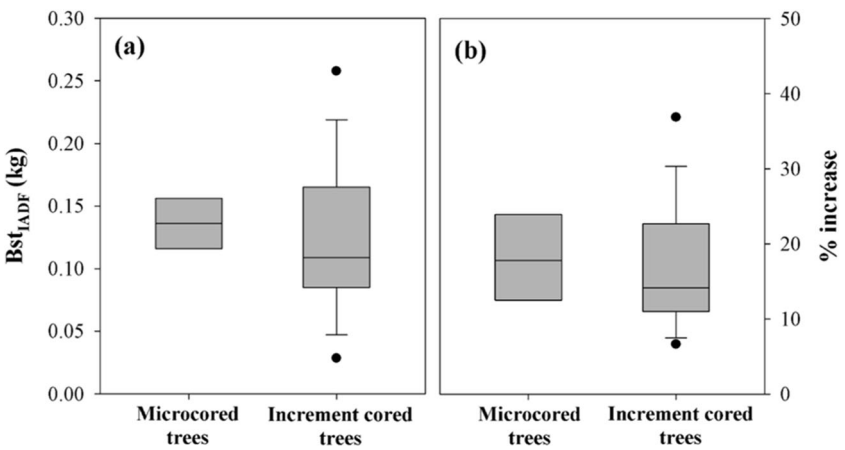

Fig. 6 Extra net (Bst_{IADF}) (**a**) and relative increase (% increase) (**b**) of the stem biomass when intra-annual density fluctuation (IADF) formation in micro-cored trees and increment-cored trees in 2016 growing season. Boxes represent upper and lower quartiles, whiskers achieve the 10th and 90th percentiles, and the mean is drawn as horizontal solid line

that a substantial proportion of trees are enough resilient to resume and extend growth if conditions return favorable.

The 1-month growth IADF-related extension in 2016 resulted in approximately 17% of additional annual stem biomass in the trees capable of resuming growth. Considering that 64% of all *J. przewalskii* trees in our study forest formed IADFs, the additional stem biomass production translates to a significant amount of carbon sequestered when compared to the less resilient non-IADF trees. Such additional growth could play an important role for forest carbon sequestration if such resilience is present in other species, at larger spatial scales, and other biomes.

5 Conclusions

Direct observations of cambial growth allowed us to identify the timing and the factors inducing IADF formation of *J. przewalskii* from a cool, arid, and continental region. Our observations indicated that precipitation during warm days in August and early September induced an additional month of growth in 64% of all trees that had stopped growing during the time of an extreme drought event. These findings both highlight the growth resilience of these trees and their flexibility to greatly extend the growing season when environmental conditions allow it. The response of trees to extreme, stressful, but transient meteorological events is one of the many uncertainties that require further study into how climatic change will impact forest ecosystems. Assessing tree species resilience to extreme event as performed in this study can provide important insight into mechanisms of growth responses that have implications for assessing forest carbon sequestration.

Acknowledgments We thank Ming Lu, Haoge Niu, and Fang Wang for their kind field work. We also thank Drs. Ben Poulter and Ruben Manzanedo for their kind comments to improve the manuscript.

Author contributions XG and NP designed the project. JZ performed field-based microcores. JZ and FZ performed lab-based experiments and data analysis. JZ drafted the manuscript, and MRA, AD, PF, and NP contributed to the final version. All authors reviewed the manuscript.

Funding This work was funded by the China Postdoctoral Science Foundation (No. 2019M653788), the National Natural Science Foundation of China (Nos. 42001043 and 41771046), the Fundamental Research Funds for the Central Universities (No. lzujbky-2019-pd04), the 111 Project (No. BP2018001), and the National Science Foundation Macrosystem Biology program (EF-1241930).

Data availability Most of the data used to support the findings of this study are included within the article; the rest are available from the corresponding author upon request.

Compliance with ethical standards

Conflict of interest The authors declare that they have no conflict of interest.

Statement on ethical approval The authors declare that they obtained the approval of the Authority of Gansu Liancheng National Nature Reserve for conducting the study in Tulugou National Forest Park.

References

Abe H, Funada R, Ohtani J, Fukazawa K (1997) Changes in the arrangement of cellulose microfibrils associated with the cessation of cell expansion in tracheids. Trees-Struct Funct 11:328–332

Balducci L, Cuny HE, Rathgeber CB, Deslauriers A, Giovannelli A, Rossi S (2016) Compensatory mechanisms mitigate the effect of warming and drought on wood formation. Plant Cell Environ 39: 1338–1352

Balzano A, Cufar K, Battipaglia G, Merela M, Prislan P, Aronne G, De Micco V (2018) Xylogenesis reveals the genesis and ecological signal of IADFs in Pinus pinea L. and Arbutus unedo L. Ann Bot 121:1231–1242

Battipaglia G, De Micco V, Brand WA, Linke P, Aronne G, Saurer M, Cherubini P (2010a) Variations of vessel diameter and delta13C in false rings of Arbutus unedo L. reflect different environmental conditions. New Phytol 188:1099–1112

Battipaglia G, De MV, Brand WA, Linke P, Aronne G, Saurer M, Cherubini P (2010b) Variations of vessel diameter and δ13C in false rings of Arbutus unedo L. reflect different environmental conditions. New Phytol 188:1099–1112

Battipaglia G, Campelo F, Vieira J, Grabner M, De Micco V, Nabais C, Cherubini P, Carrer M, Brauning A, Cufar K, Di Filippo A, Garcia-Gonzalez I, Koprowski M, Klisz M, Kirdyanov AV, Zafirov N, de Luis M (2016) Structure and function of intra-annual density fluctuations: mind the gaps. Front Plant Sci 7:595

Bunn AG, Waggoner LA, Graumlich LJ (2005) Topographic mediation of growth in high elevation foxtail pine (Pinus balfouriana Grev. et Balf.) forests in the Sierra Nevada, USA. Glob Ecol Biogeogr 14: 103–114

Campelo F, Nabais C, Freitas H, Gutiérrez E (2007) Climatic significance of tree-ring width and intra-annual density fluctuations in Pinus pinea from a dry Mediterranean area in Portugal. Ann Forest Sci 64:229–238

Campelo F, Vieira J, Nabais C (2013) Tree-ring growth and intra-annual density fluctuations of Pinus pinaster responses to climate: does size matter? Trees 27:763–772

Copenheaver CA, Pokorski EA, Currie JE, Abrams MD (2006) Causation of false ring formation in Pinus banksiana: a comparison of age, canopy class, climate and growth rate. Forest Ecol Manag 236:348–355

Cuny HE, Fonti P, Rathgeber CBK, von Arx G, Peters RL, Frank DC (2019) Couplings in cell differentiation kinetics mitigate air temperature influence on conifer wood anatomy. Plant Cell Environ 42: 1222–1232

De Grandpré L, Tardif JC, Hessl A, Pederson N, Conciatori F, Green TR, Oyunsanaa B, Baatarbileg N (2011) Seasonal shift in the climate responses of Pinus sibirica, Pinus sylvestris, and Larix sibirica trees from semi-arid, north-central Mongolia. Can J For Res 41:1242–1255

De Micco V, Balzano A, Cufar K, Aronne G, Gricar J, Merela M, Battipaglia G (2016a) Timing of false ring formation in Pinus halepensis and Arbutus unedo in Southern Italy: outlook from an analysis of xylogenesis and tree-ring chronologies. Front Plant Sci 7: 705

De Micco V, Campelo F, De Luis M, Bräuning A, Grabner M, Battipaglia G, Cherubini P (2016b) Intra-annual density fluctuations in tree rings: how, when, where, and why? IAWA J 37:232–259

Deslauriers A, Huang JG, Balducci L, Beaulieu M, Rossi S (2016) The contribution of carbon and water in modulating wood formation in black spruce saplings. Plant Physiol 170:2072–2084

Deslauriers A, Fonti P, Rossi S, Rathgeber C, Gričar J (2017) Ecophysiology and plasticity of wood and phloem formation. In: AmorosoLori MM, Daniels LD, Baker PJ, Camarero JJ (eds) Dendroecology, Tree-ring analyses applied to ecological studies. Springer International Publishing, pp 13–33

Edmondson JR (2010) The meteorological significance of false rings in Eastern Redcedar (Juniperus virginiana L.) from the Southern Great Plains, U.S.A. Tree-Ring Res 66:19–33

Fang J, Chen A, Peng C, Zhao S, Ci L (2001) Changes in forest biomass carbon storage in China between 1949 and 1998. Science 292:2320–2322

Fernandez-de-Una L, Rossi S, Aranda I, Fonti P, Gonzalez-Gonzalez BD, Canellas I, Gea-Izquierdo G (2017) Xylem and leaf functional adjustments to drought in Pinus sylvestris and Quercus pyrenaica at their elevational boundary. Front Plant Sci 8:1200

Fonti P, von Arx G, Garcia-Gonzalez I, Eilmann B, Sass-Klaassen U, Gartner H, Eckstein D (2010) Studying global change through investigation of the plastic responses of xylem anatomy in tree rings. New Phytol 185:42–53

García Morote FA, López Serrano FR, Andrés M, Rubio E, González Jiménez JL, de las Heras J (2012) Allometries, biomass stocks and biomass allocation in the thermophilic Spanish juniper woodlands of Southern Spain. Forest Ecol Manag 270:85–93

Gou X, Deng Y, Gao L, Chen F, Cook E, Yang M, Zhang F (2015) Millennium tree-ring reconstruction of drought variability in the eastern Qilian Mountains, Northwest China. Clim Dynam 45: 1761–1770

Kumagai T, Saitoh TM, Sato Y, Morooka T, Manfroi OJ, Kuraji K, Suzuki M (2004) Transpiration, canopy conductance and the decoupling coefficient of a lowland mixed dipterocarp forest in Sarawak, Borneo: dry spell effects. J Hydrol 287:237–251

Lloyd AH, Sullivan PF, Bunn AG (2017) Integrating dendroecology with other disciplines improves understanding of upper and latitudinal treelines. In: AmorosoLori M, Daniels L, Baker P, Camarero J (eds) Dendroecology, Tree-Ring Analyses Applied to Ecological Studies. Springer International Publishing, pp 135–157

Marchand N, Filion L (2012) False rings in the white pine (Pinus strobus) of the Outaouais Hills, Québec (Canada), as indicators of water stress. Can J For Res 42:12–22

Masiokas M, Villalba R (2004) Climatic significance of intra-annual bands in the wood of Nothofagus pumilio in southern Patagonia. Trees 18:696–704

McDowell NG, Allen CD (2015) Darcy's law predicts widespread forest mortality under climate warming. Nat Clim Chang 5:669–672

Muller B, Pantin F, Génard M, Turc O, Freixes S, Piques M, Gibon Y (2011) Water deficits uncouple growth from photosynthesis, increase C content, and modify the relationships between C and growth in sink organs. J Exp Bot 62:1715–1729

Novak K, de Luís M, Raventós J, Čufar K (2013) Climatic signals in tree-ring widths and wood structure of Pinus halepensis in contrasted environmental conditions. Trees 27:927–936

Novak K, de Luis M, Saz MA, Longares LA, Serrano-Notivoli R, Raventos J, Cufar K, Gricar J, Di Filippo A, Piovesan G, Rathgeber CB, Papadopoulos A, Smith KT (2016) Missing rings in Pinus halepensis - the missing link to relate the tree-ring record to extreme climatic events. Front Plant Sci 7:727

Oribe Y, Funada R, Kubo T (2003) Relationships between cambial activity, cell differentiation and the localization of starch in storage tissues around the cambium in locally heated stems of Abies sachalinensis (Schmidt) Masters. Trees-Struct Funct 17:185–192

Pan Y, Birdsey RA, Fang J, Houghton R, Kauppi PE, Kurz WA, Phillips OL, Shvidenko A, Lewis SL, Canadell JG, Ciais P, Jackson RB, Pacala SW, McGuire AD, Piao S, Rautiainen A, Sitch S, Hayes D (2011) A large and persistent carbon sink in the world's forests. Science 333:988–993

Popkova MI, Vaganov EA, Shishov VV, Babushkina EA, Rossi S, Fonti MV, Fonti P (2018) Modeled tracheidograms disclose drought influence on Pinus sylvestris tree-rings structure from Siberian forest-steppe. Front Plant Sci 9:1144

Ren P, Rossi S, Camarero JJ, Ellison AM, Liang E, Penuelas J (2018) Critical temperature and precipitation thresholds for the onset of xylogenesis of Juniperus przewalskii in a semi-arid area of the north-eastern Tibetan Plateau. Ann Bot 121:617–624

Rigling A, Waldner PO, Forster T, Bräker OU, Pouttu A (2001) Ecological interpretation of tree-ring width and intraannual density fluctuations in Pinus sylvestris on dry sites in the central Alps and Siberia. Can J For Res 31:18–31

Rossi S, Anfodillo T, Menardi R (2006) Trephor: a new tool for sampling microcores from tree stems. IAWA J 27:89–97

Rossi S, Anfodillo T, Čufar K, Cuny HE, Deslauriers A, Fonti P, Frank D, Gricar J, Gruber A, Huang JG, Jyske T, Kaspar J, King G, Krause C, Liang E, Makinen H, Morin H, Nojd P, Oberhuber W, Prislan P, Rathgeber CB, Saracino A, Swidrak I, Treml V (2016) Pattern of xylem phenology in conifers of cold ecosystems at the Northern Hemisphere. Glob Chang Biol 22:3804–3813

Sanchez-Salguero R, Camarero JJ, Gutierrez E, Gonzalez Rouco F, Gazol A, Sanguesa-Barreda G, Andreu-Hayles L, Linares JC, Seftigen K (2017) Assessing forest vulnerability to climate warming using a process-based model of tree growth: bad prospects for rear-edges. Glob Chang Biol 23:2705–2719

Schulman E (1939) Classification of false annual rings in west Texas pine. Tree-Ring Bull 6:11–13

Stokes M, Smiley T (1968) An introduction to tree-ring dating

Vieira J, Rossi S, Campelo F, Freitas H, Nabais C (2014) Xylogenesis of Pinus pinaster under a Mediterranean climate. Ann Forest Sci 71: 71–80

Wang L, Payette S, Bégin Y (2000) A quantitative definition of light rings in black spruce (Picea mariana) at the arctic treeline in northern Québec, Canada. Arct Antarct Alp Res 32:324–330

Zhang J (2018) Cambial phenology and intra-annual radial growth dynamics of conifers over the Qilian Mountains. vol Doctor. Lanzhou University, Lanzhou

Zhang J, Gou X, Zhao Z, Liu W, Zhang F, Cao Z, Zhou F (2013) Improved method of obtaining micro-core paraffin sections in Dendroecological research. Chin J Plant Ecol 37:972–978

Zhang J, Gou X, Manzanedo RD, Zhang F, Pederson N (2018) Cambial phenology and xylogenesis of Juniperus przewalskii over a climatic gradient is influenced by both temperature and drought. Agric For Meteorol 260-261:165–175

Publisher's note Springer Nature remains neutral with regard to jurisdictional claims in published maps and institutional affiliations.